EUROPEAN FUSION DEVELOPMENT AGREEMENT

EFDA-JET-CP(05)02-24

G.M.D. Hogeweij, H.J. de Blank, C. Bourdelle, N. Hawkes, F. Imbeaux,
N. Kirneva and JET EFDA contributors

Analysis of Electron Internal Transport Barriers in JET Low and Reversed Shear Discharges

Analysis of Electron Internal Transport Barriers in JET Low and Reversed Shear Discharges

G.M.D. Hogeweij[1], H.J. de Blank[1], C. Bourdelle[2], N. Hawkes[3], F. Imbeaux[2], N. Kirneva[4] and JET EFDA contributors*

[1]FOM Institute for Plasma Physics Rijnhuizen, Association EURATOM-FOM, Trilateral Euregio Cluster, P.O.Box 1207, Nieuwegein, The Netherlands
[2]Association EURATOM -CEA, CEA Cadarache, 13108 St Paul-Lez-Durance, France
[3]EURATOM/UKAEA Fusion Association, Culham Science Centre, Abingdon, OX14 3DB, UK
[4]Nuclear Fusion Institute, RRC Kurchatov Institute, Moscow, Russia
** See annex of J. Pamela et al, "Overview of JET Results ", (Proc.20 th IAEA Fusion Energy Conference, Vilamoura, Portugal (2004).*

Preprint of Paper to be submitted for publication in Proceedings of the EPS Conference,
(Tarragona, Spain 27th June - 1st July 2005)

INTRODUCTION.

The study of electron thermal transport and electron Internal Transport Barriers (eITBs) in regimes with dominant electron heating is of great importance for ITER. Single JET pulses with eITB were studied in [1,2]. In this paper for the first time a consistent study of 15 predominantly electron heated JET pulses with and without eITB is presented, covering the full range of safety factor (q) profiles, from strongly reversed shear (s) via low shear to standard positive shear. The difference in q profiles is mainly brought about by the use of various Lower Hybrid (LH) power levels.

The presence of eITBs in the experiments is analyzed in two ways. First, local reduction of electron thermal diffusion is searched for by means of local power balance analysis, performed with the CRONOS code [3]. CRONOS is also used to calculate the current driven by LH, which is an essential ingredient to calculate q. For many pulses no or very limited Motional Stark Effect data (from which q is derived) are present; when MSE data are available, they will be compared with the CRONOS calculations.

Second, the so-called ρ_T* ITB analysis [4] is used; here an eITB manifests itself as a local enhancement of the dimensionless parameter $\rho_{Te}^* = \rho_s/L_{Te}$, where ρ_s is the ion Larmor radius at sound speed and L_{Te} the local T_e gradient scale length.

Linear microstability analysis with KineZero [5] is performed for these pulses to assess linear growth rates (γ_{lin}) in both the ITG-TEM and ETG range of wavelengths.

This paper addresses the following questions:

- Dependence of sustainment and quality of eITB on s.
- Relation between experimentally observed eITB and stabilization of instabilities.
- Parametric dependence of γ_{lin} on plasma parameters, in particular s and the T_e inverse gradient length (A_{Te}).

2. eITB ANALYSIS AND RELATION WITH MAGNETIC SHEAR

As typical for the dataset, the JET Pulse No's: 62796/97 are compared, which had the same scenario apart from LH power, see Fig.1. The ρ_T* eITB analysis, plotted in Fig.2, shows a clear difference between the two pulses: whereas 62797 loses the eITB after the preheat phase, 62796 sustains the eITB in the current flat top phase, albeit at a smaller radius than in the preheat phase.

Figure 3 shows the profiles of χ_e, q, s (as calculated by CRONOS), q from MSE, and ρ_{Te}* for these two pulses during the steady state phase at 8s. The q profiles from MSE are in fair agreement with q from CRONOS: for 62797 both are monotonic; for 62796 both have a minimum at nearly the same position. At this time the eITB is only present in 62796, i.e. in the pulse with reversed shear, and located just inside qmin. Note the good match of maximum ρ_{Te}* and minimum χ_e for pulse 62796. In the preheat phase (not shown here) both pulses have an eITB and reversed shear.

3. LINK BETWEEN eITB OBSERVATION AND SUPPRESSION OF INSTABILITIES.

In most cases suppression of the ITG-TEM branch of microturbulence, as calculated with KineZero, corresponds fairly well with the presence of an eITB. Figure 4 compares ρ_{Te}* with $\gamma^{ITG\text{-}TEM}$ for the

two pulses analyzed in the previous section, plus Pulse No:53510, which will be analyzed further on. The presence/absence of an eITB inside $\rho = 0.3$ for 62796/97 is reflected in absence/presence of turbulence in the same region. For pulse 53510, the area of suppressed instabilities lies at somewhat larger radius than the eITB. The ETG branch of turbulence (not shown here) generally only plays a role in the outer part of the plasma ($\rho > 0.7$).

3. LINK BETWEEN S AND SUPPRESSION OF INSTABILITIES

This is tested starting from JET Pulse No: 53510, which had a well-established eITB. Figure 5 shows the time evolution of the maximum value of $\rho_{Te}*$ ($\rho_{Te}*^{max}$), its position ρ ($\rho_{Te}*^{max}$), the position of q_{min}, as calculated by CRONOS, q_{min}, and the input power levels. The eITB resides at "C 10% smaller radius than qmin. The single MSE data point available is also plotted (asterisks), and shows satisfactory agreement with the CRONOS result.

Then figure 6 shows the KineZero calculations of $\gamma^{ITG\text{-}TEM}$ and γ^{ETG}. KineZero was run for the profiles as calculated by CRONOS (blue) and for cases with artificially de- creased (violet) and increased s (green, red). It is clearly seen that the level of ITG-TEM turbulence in the eITB region ($\rho \sim 0.2-0.4$) strongly depends on s: the turbulence is strongly enhanced for positive s, and is further suppressed for more negative s.

4. KINEZERO STUDY OF ATE DEPENDENCE OF TURBULENCE

The analysis of the dependence of microturbulence on inverse gradient length (A_{Te}) is done starting again from Pulse No: 53510. A_{Te} is doubled and halved for both the experimental s profile, and for an artificial monotonic s profile; T_e itself is left unchanged, so this is really a test of the effect of local steepening of ∇Te. The results are shown in figure 7. In the eITB region the ITG-TEM turbulence is insensitive for A_{Te} ; in contrast, for positive s, a strong increase of microturbulence with A_{Te} is

CONCLUSIONS

In the type of pulses studied, i.e. with dominant e heating and low momentum input, eITB strength is mainly determined by s. Considering the whole dataset (now shown here), there appears to be no sharp transition between plasmas with and without eITB.

MSE data availability for the present dataset is scarce. When available, the MSE data are in good agreement with the CRONOS calculations; this gives us confidence that we can rely on the CRONOS results also for cases where MSE is not available.

The experimental signatures of eITBs correspond well with the findings of microstability calculations. Moreover, these calculations confirm the central role of s. This role of negative s in ITB formation corroborates results of turbulent transport modeling [6]. With negative shear, increasing inverse gradient length does not enhance the turbulence - a true sign of an ITB.

ACKNOWLEDGEMENTS

This work, supported by the European Communities under the contract of Association between EURATOM/FOM, was carried out within the framework of the European Fusion Programme with financial support from NWO. The views and opinions expressed herein do not necessarily reflect those of the European Commission.

REFERENCES

[1]. Hogeweij G.M.D. et al, Plasma Phys. Contr. Fusion **42** (2002) 1155

[2]. Kirneva N. et al, Controlled Fusion and Plasma Physics (Proc. 31th Eur. Conf., London, UK, 2004), CD-ROM file P-1.152

[3]. Basiuk V. et al, Nucl. Fusion **43** (2003) 822

[4]. Tresset G. et al, Nucl. Fusion **42** (2002) 520

[5]. Bourdelle C. et al, Nucl. Fusion **42** (2002) 892

[6]. Baranov Yu. et al, Plasma Phys. Contr. Fusion **46** (2004) 1181

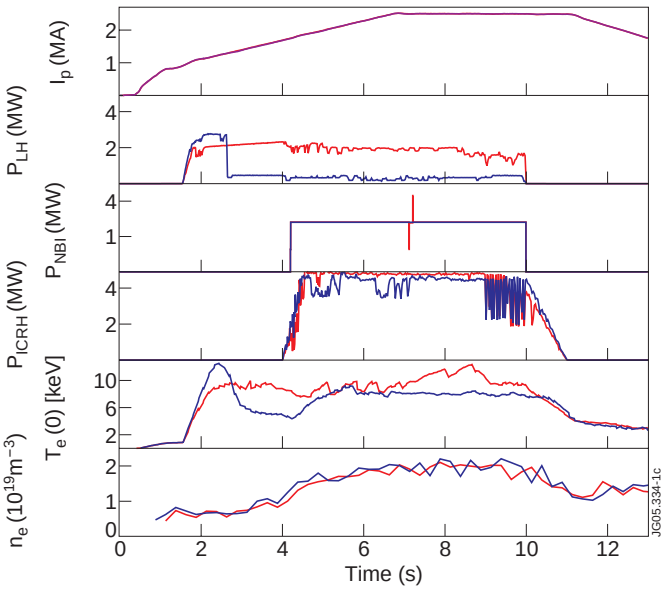

Figure 1: Scenario of JET Pulse No's: 62796 and 62797: the panels show the time evolution of I_p, P_{LH}, P_{NBI}, P_{ICRH}, $T_e(0)$, and ne.

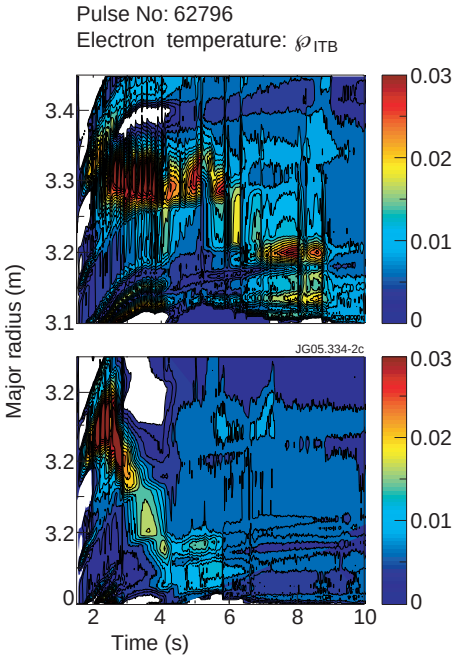

Figure 2: ρ_T electron ITB analysis for the two pulses of Fig.1, showing a striking difference in evolution. The colours indicate the value of ρ_{Te}*; a value of 0.014 is considered as ITB margin.*

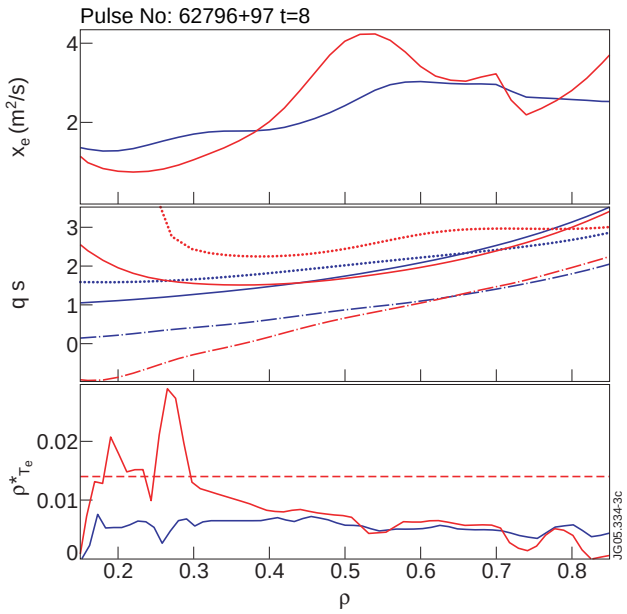

Figure 3: Profiles for Pulse No's: 62796 and 62797 at 8s. Upper panel: χ_e; middle panel: q (full) and s (dashed lines) as calculated by CRONOS, and q from MSE (dotted lines); lower panel: ρ_{Te}.*

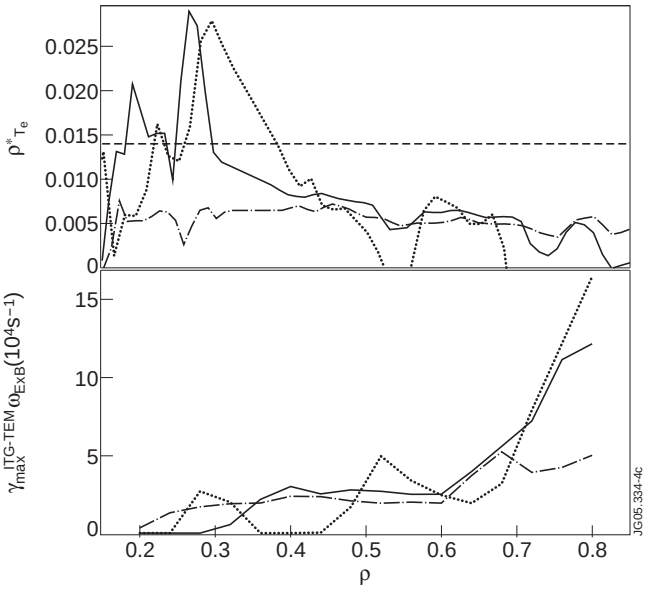

Figure 4: Profiles of ρ_{Te} (upper panel) and $\gamma^{ITG"TEM}_{max}$ (lower panel) for Pulse No's: 53510, 62796 and 62797 at 8s.*

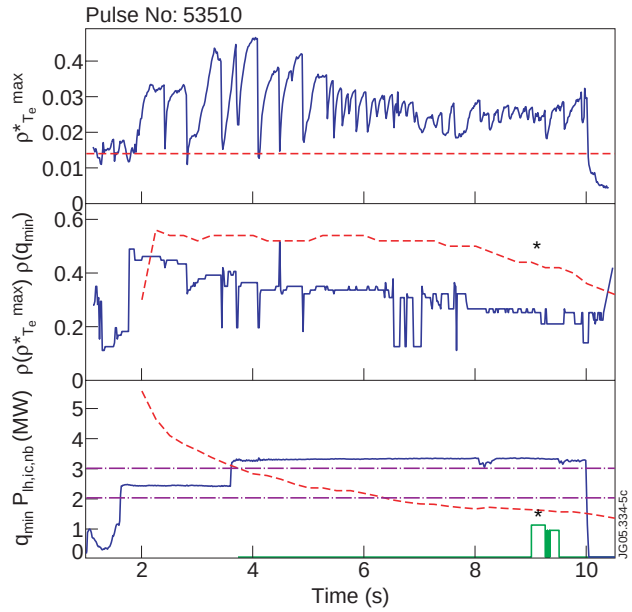

Figure 5: Time traces for Pulse No: 53510. Upper: ρ_{Te} ^{max} and ITB criterion; middle: ρ (ρ_{Te}* ^{max}) and (q_{min}) (from CRONOS); lower: qmin (from CRONOS), P_{LH} and P_{NBI}. In this pulse there was only a short NBI blip, resulting in just 1 MSE data point; the asterisks in the 2nd and 3rd panel indicate ρ (q_{min}) and q_{min} from MSE.*

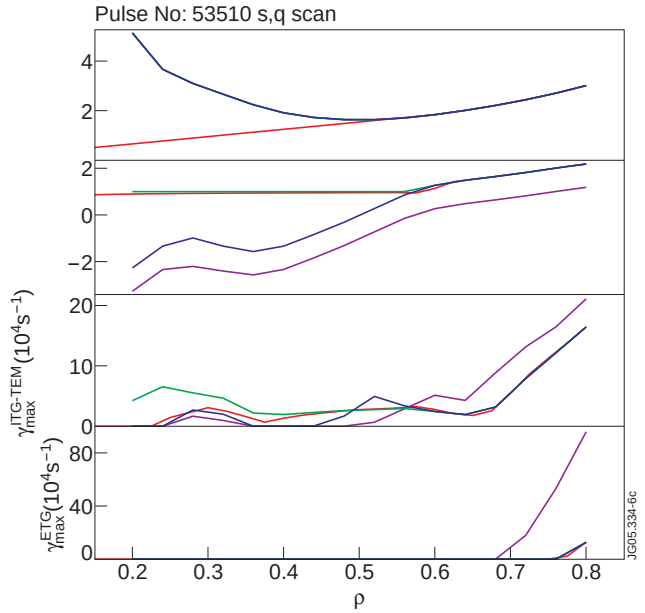

Figure 6: KineZero microstability calculations for Pulse No: 53510 at t = 8s (blue), and for cases with artificially decreased s (violet), and increased s (green with unchanged q; red with consistently changed q).

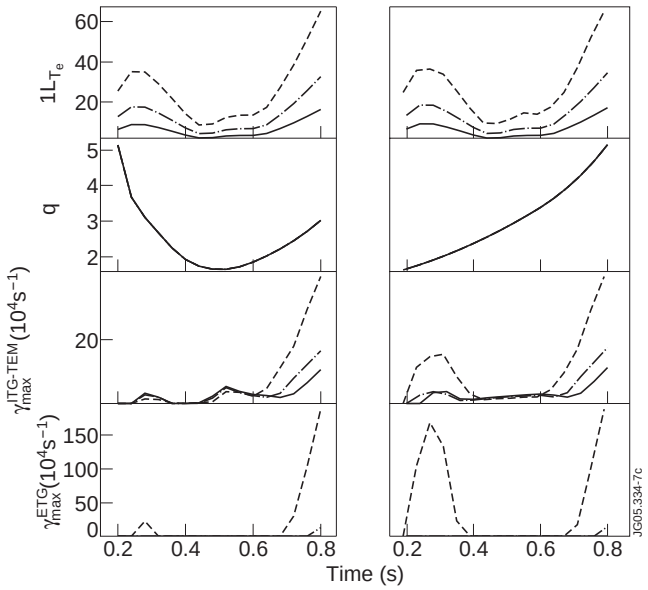

Figure 7: KineZero study of A_{Te} dependence of turbulence, based on Pulse No: 53510, for (left) experimental q and (right) monotonic q. 1st panel: A_{Te} 2nd: q; 3rd: $\gamma_{max}^{ITG-TEM}$; 4th: γ_{max}^{ETG}. Shown are results for experimental, doubled and halved A_{Te}.